# The dynamics of a symmetric coupling of three modified quadratic maps*

Paulo C. Rech†

*Departamento de Física, Universidade do Estado de Santa Catarina, 89219-710 Joinville, Brazil*

(Received 22 October 2012; revised manuscript received 26 January 2013)

We investigate the dynamical behavior of a symmetric linear coupling of three quadratic maps with exponential terms, and identify various interesting features as a function of two control parameters. In particular, we investigate the emergence of quasiperiodic states arising from Naimark–Sacker bifurcations of stable period-1, period-2, and period-3 orbits. We also investigate the multistability in the same coupling. Lyapunov exponents, parameter planes, phase space portraits, and bifurcation diagrams are used to investigate transitions from periodic to quasiperiodic states, from quasiperiodic to mode-locked states and to chaotic states, and from chaotic to hyperchaotic states.

**Keywords:** Naimark–Sacker bifurcation, quasiperiodicity, chaos, hyperchaos

**PACS:** 02.30.Rz, 05.45.−a **DOI:** 10.1088/1674-1056/22/8/080202

## 1. Introduction

Discrete-time models, as discrete maps consisting of difference equations, are commonly associated with real nonlinear dynamical systems. For example, the Hénon map[1] is useful to model $CO_2$ lasers in the limit of strong dissipation,[2] and also to numerically demonstrate the validity of secure digital chaotic communication based on contraction maps,[3] just to mention a few uses of this paradigmatic model. In another example, a two-parameter family of one-dimensional maps was proposed by Colli and co-workers[4] to model the bubble formation in an experiment that considers the air injection in a liquid. Other examples involve the modeling of the population growth of insects in a limited environment,[5] a discrete model of a two-gene system,[6] whose associated two-dimensional map was derived from chemical reactions corresponding to gene expression and regulation, coupled maps to model traffic flow,[7] and a chaos-based cryptosystem for fractal image coding.[8] Generally speaking, maps have received much attention in recent times, because of their application in a great number of practical systems, in many fields.[9]

In this paper we introduce a discrete-time system, namely a linear symmetric coupling of three quadratic maps, each having an exponential term, given by

$$\begin{aligned} x_{n+1} &= b\left(\mathrm{e}^{-50x_n^2} - x_n^2\right) + a y_n, \\ y_{n+1} &= b\left(\mathrm{e}^{-50y_n^2} - y_n^2\right) + a z_n, \\ z_{n+1} &= b\left(\mathrm{e}^{-50z_n^2} - z_n^2\right) + a x_n, \end{aligned} \tag{1}$$

where $x_n$, $y_n$, $z_n$ represent dynamical variables, $b$ is the control parameter of the individual quadratic map with exponential term, $a$ is the coupling parameter, and $n = 0, 1, 2, \ldots$ is the discrete time. As we will see in the sequence, this model presents very complex dynamics in the $b \times a$ parameter plane, including regions characterized by periodic, quasiperiodic, mode-locked, chaotic, and hyperchaotic states.

We would like to point out that the dynamics of a quadratic map with an exponential term were recently investigated by Bao and co-workers.[10] By using bifurcation diagrams and phase-space trajectories, the authors showed that the model has a dynamical behavior similar to that presented by the original quadratic map, including a route to chaos via period-doubling bifurcations. A particular coupling of two quadratic maps with exponential terms was also investigated, with a different route to chaos being detected, namely a route via quasiperiodicity in consequence of Naimark–Sacker bifurcations (NSb).[11,12] More recently, the dynamics of a two-dimensional map, equivalent to the coupling of two quadratic maps with exponential terms, were investigated by Li and co-workers.[13]

## 2. Results and discussion

Figure 1 shows a global view of the $b \times a$ parameter plane of system (1). It is an isoperiodic diagram obtained by discretizing the parameter interval in a grid of $500 \times 500$ points equally spaced. For each point $(a, b)$, an orbit of initial condition $(x_0, y_0, z_0) = (0.1, 0.3, 0.5)$ converges to a hyperchaotic, or to a chaotic, or to a quasiperiodic, or to a periodic attractor, or to an attractor at infinity (an unbounded attractor), after a transient of $5 \times 10^4$ iterates. If the trajectory initialized in $(x_0, y_0, z_0)$ converges to infinity, that is diverges, we try until 500 new initializations, always increasing by 1/500 each one of the variables. In Fig. 1 parameters for which the trajec-

*Project supported by Conselho Nacional de Desenvolvimento Científico e Tecnológico-CNPq, Brazil.

†Corresponding author. E-mail: dfi2pcr@joinville.udesc.br

© 2013 Chinese Physical Society and IOP Publishing Ltd 

tories escape to infinity (converge to the unbounded attractor) are related with the blank region, and parameters for which the trajectories converge to attractors with periodicities between 5 and 50 are painted in black. Some periodic regions are identified by integer numbers, which denote the period of the respective region. Chaotic, hyperchaotic, and quasiperiodic regions are identified by the letters C, H, and Q, respectively. As can be seen in Fig. 1, periodic or non-periodic regions are symmetrically organized in the parameter plane. This happens because when we change $b$ by $-b$, the map (1) remains invariant through an exchange of $x$ by $-x$, $y$ by $-y$, and $z$ by $-z$.

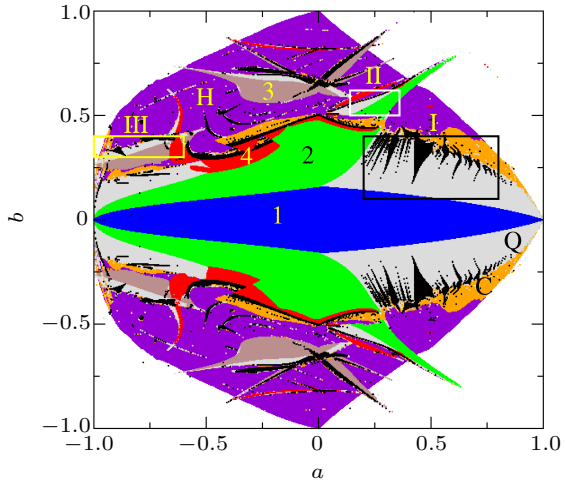



**Fig. 1.** (color online) The $b \times a$ parameter plane of the coupling (1). In this and further similar plots, domains of different attractors are identified by different shadings. Numbers indicate periods and letters indicate chaos (C), hyperchaos (H), and quasiperiodicity (Q).

Panels in Fig. 2 show the magnification of three disconnected regions with quasiperiodic behavior, in gray in Fig. 1, two of them being inhabited by resonance regions in black, which are periodic regions similar to Arnold tongues observed in the circle map.[14] Figure 2(a) (magnification of the boxed region I in Fig. 1) illustrates in gray a parameter region for which a quasiperiodic motion is born on the boundary with the period-1 region in blue. For parameter values taken along this boundary line between gray and blue regions, Naimark–Sacker bifurcations[11,12] (NSb) occur. This means that inside the gray region in Fig. 2(a) we have quasiperiodic motion with one invariant closed curve, originated from a fixed point. Embedded in this quasiperiodic region, we can see an infinite number of periodic structures in black, similar to Arnold tongues and with the most varied periods.

Figure 2(b) (magnification of the boxed region II in Fig. 1) illustrates in gray a parameter region for which a quasiperiodic motion is born on the boundary with the period-2 region in green. Now, for parameter values taken along the boundary line between gray and green regions NSb occur, so that within the gray region we have quasiperiodic motion with

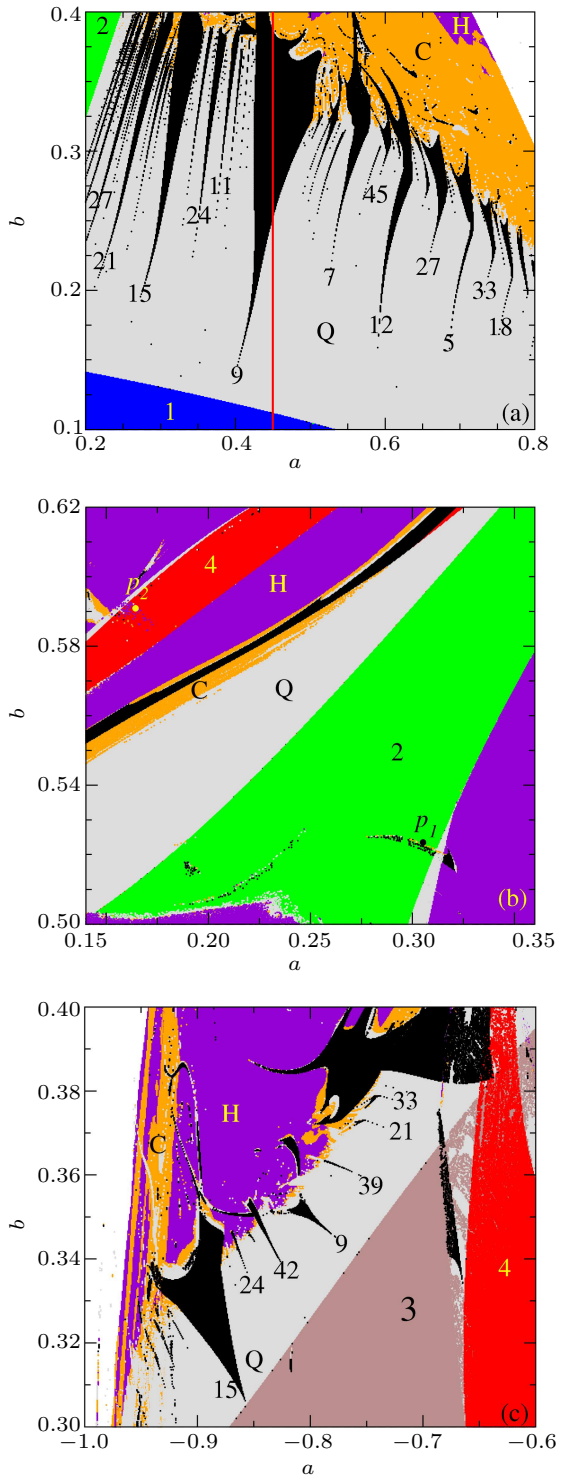



**Fig. 2.** (color online) (a) Magnification of the box I in Fig. 1. (b) Magnification of the box II in Fig. 1. (c) Magnification of the box III in Fig. 1. For parameters in the neighborhood of $p_1$ and $p_2$ in panel (b), multistability takes place (see the text).

two invariant closed curves, now originated from a period-2 orbit. Unlike before, this time periodic structures embedded in the quasiperiodic region do not appear. Figure 2(c) (magnification of the boxed region III in Fig. 1) illustrates in gray a parameter region for which a quasiperiodic motion is born on the boundary with the period-3 region in brown. This time,

for parameter values taken along the boundary line between gray and brown regions, NSb occur from a period-3 orbit and, therefore, within the gray region we have quasiperiodic motion with three invariant closed curves. Again periodic structures appear embedded in the quasiperiodic region. As is known,[12] these periodic structures embedded in the quasiperiodic region have self-similar properties with pattern repetition in different length scales. This fact can be checked in two panels of Fig. 2, namely those shown in Figs. 2(a) and 2(c).

In the sequel we will concentrate in Fig. 2(a), to investigate details on the dynamics of the system (1). However, it is important to note that investigation with similar results may also be made by considering Fig. 2(b) or 2(c). Such findings, related to Figs. 2(b) and 2(c), are not included here to avoid repetition. Figure 3 shows in panel (a) the bifurcation diagram ($x$ variable), and in panel (b) the largest (continuous line) and the second largest (dashed line) Lyapunov exponent ($\lambda$) plots, both for $a = 0.45$ and $0.1 < b < 0.4$, i.e., both for points along the red line in Fig. 2(a). For the construction of the bifurcation diagram, $10^3$ values of the parameter $b$ were considered, and we plotted 50 points for each one of them, after a transient of $5 \times 10^4$ iterates, always from the initial condition ($x_0$, $y_0$, $z_0$). The same initial condition, transient, and discretization in the $b$ axis were considered for the construction of the largest and the second largest Lyapunov exponent plots, each $\lambda$ value being obtained by averaging over $10^6$ iterations.

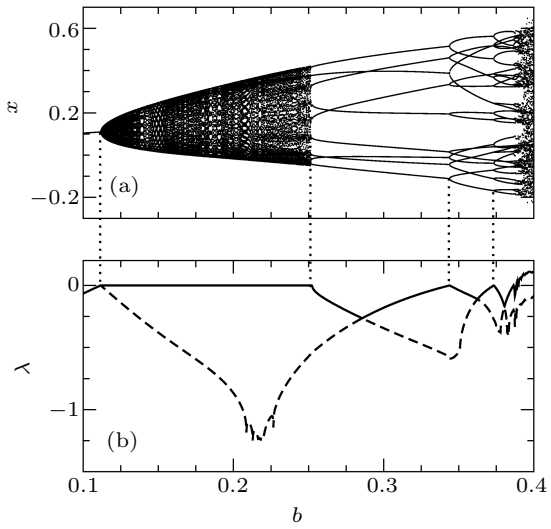



**Fig. 3.** (a) Bifurcation diagram showing the variable $x$. (b) The largest (continuous line) and the second largest (dashed line) Lyapunov exponent plots. Both graphs as a function of the parameter $b$, for $a = 0.45$.

By increasing $b$ from 0.1 along the red line $a = 0.45$ in Fig. 2(a), the system stays in a period-1 state until $b \approx 0.11$, being characterized by a largest Lyapunov exponent less than zero. At $b \approx 0.11$, the largest Lyapunov exponent reaches the zero value, and a quasiperiodic region is attained, remaining until $b \approx 0.39$. This quasiperiodic motion is, therefore,

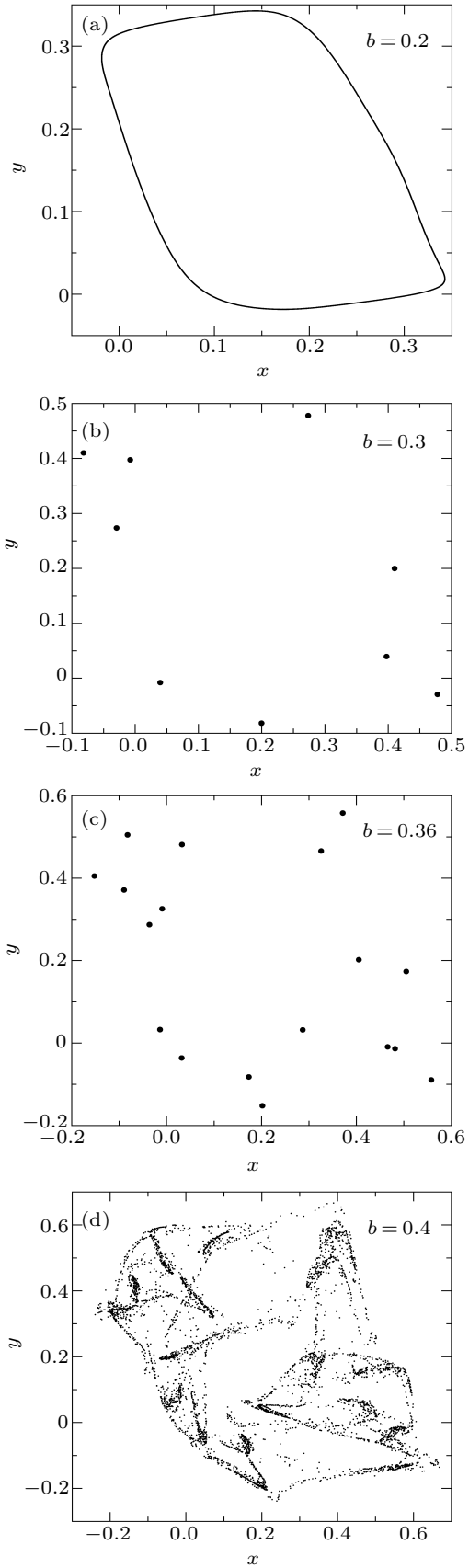



**Fig. 4.** Projections in the $xy$ plane of four trajectories in the three-dimensional phase-space of system (1) showing: (a) quasiperiodicity for $a = 0.45$, $b = 0.2$, (b) a period-9 orbit for $a = 0.45$, $b = 0.3$, (c) a period-18 orbit for $a = 0.45$, $b = 0.36$, and (d) chaos for $a = 0.45$, $b = 0.4$. Same initial conditions and transient of the other figures were utilized in each panel, being plotted $5 \times 10^3$ points.

originated from a period-1 orbit, and is a consequence of an NSb that occurs at $b \approx 0.11$. As a result of this NSb, one invariant closed curve is created in the $xyz$ phase-space, whose typical example can be seen in Fig. 4(a), that shows an $xy$ projection of the three-dimensional quasiperiodic attractor for $a = 0.45$, $b = 0.2$. There are mode-locked states (Arnold tongues) embedded in the quasiperiodic region, for which the largest Lyapunov exponent is less than zero. By increasing $b$ from 0.11 along the red line $a = 0.45$ in Fig. 2(a), we cross the quasiperiodic region and penetrate a period-9 tongue at $b \approx 0.25$. Period-doubling bifurcations happen at $b \approx 0.34$ and $b \approx 0.37$, resulting in period-18 and period-36 orbits, respectively. Examples of these periodic orbits can be seen in Figs. 4(b) and 4(c), respectively period-9 for $b = 0.3$ and period-18 for $b = 0.36$. By increasing $b$ more, finally a chaotic state for which the largest Lyapunov exponent is greater than zero is created at $b \approx 0.39$. A typical chaotic attractor appears in Fig. 4(d), for $a = 0.45$, $b = 0.4$. We would like to point out that system (1) may also present hyperchaotic states, whose regions in panels of Figs. 1 and 2 appear in violet.

Up to now, in this paper, the dynamics of the coupling (1) were visualized by using parameter planes, bifurcation diagrams, Lyapunov exponents plots, and selected cross sections of the three-dimensional phase-space. Now we are interested in the investigation of multistability, whose significance is related to the possibility of existence of more than one dynamic state, for a same parameter set. Superimposed colors in the neighborhood of points $p_1 = (a_1, b_1) = (0.301627, 0.522755)$ and $p_2 = (a_2, b_2) = (0.160674, 0.59012)$ in the parameter plane of Fig. 2(b) are a strong indication of multistability. Panels in Fig. 5 illustrate $z = 0.2$ cross sections of basins of attraction for the coupling (1), with the parameters being related to point $p_1$ in the panel (a), and to point $p_2$ in the panel (b). We consider $250 \times 10^3$ initial conditions for the construction of each panel. As is known, basins of attraction make it possible to separate attractors in the phase-space by coloring different dynamical behaviors differently. Black and white in panel (a) in Fig. 5 represent, respectively, the basins of attraction corresponding to the set of initial conditions that leads system (1) to a period-2 attractor and to a period-12 attractor. Meanwhile, black and white in panel (b) in Fig. 5 represent, respectively, the basins of attraction corresponding to the set of initial conditions that leads system (1) to a period-4 attractor and to a hyperchaotic attractor. The basin of the period-2 attractor is much greater than the basin of the period-12 attractor, the first being composed of about 76% of the points that compose the whole basin. Something similar happens when we confront the basins of the period-4 and the hyperchaotic attractor. In this case, the basin of the period-4 attractor is composed of about 88% of the points that compose the whole basin. Roughly, both panels in Fig. 5 can be interpreted as showing a large black area, riddled with white dots.

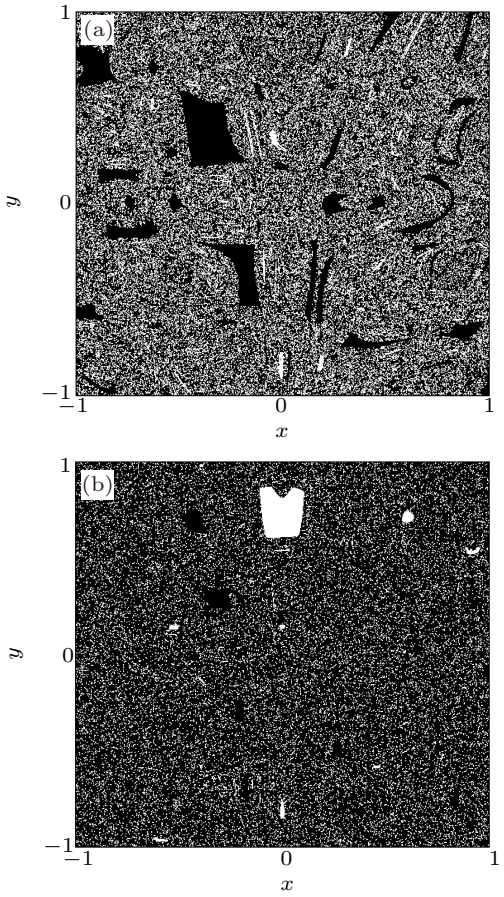



**Fig. 5.** Basins of attraction sections for the coupling (1). Black (white) is the basin of the period-2 (period-12) attractor in panel (a), while black (white) is the basin of the period-4 (hyperchaotic) attractor in panel (b).

## 3. Summary

In this paper we have considered a three-dimensional dynamical system with a quadratic nonlinearity, which consists in a symmetric linear coupling of three quadratic maps with exponential terms. We have shown that this system may exhibit several routes to chaos via quasiperiodicity, on account of Naimark–Sacker bifurcations from period-1, period-2, and period-3 orbits. We have identified the coexistence of two attractors for the same set of parameters, phenomenon known as multistability. Numerical results, including Lyapunov exponents, parameter plane and phase-space plots, bifurcation diagrams, and basins of attraction were used to describe the nonlinear dynamics of the coupling. Although we have considered a simple system of only three coupled maps, we believe that similar results can be obtained for more general systems, namely, for an array of coupled quadratic maps with exponential terms. We argue that hyperchaos may be more easily reached, because with the increasing of the system dimension, increases the possibility of the system having more than one positive Lyapunov exponent.

## References


[1] Hénon M 1976 *Commun. Math. Phys.* **50** 69
[2] Pando C L, Acosta G A L, Meucci R and Ciofini M 1995 *Phys. Lett. A* **199** 191
[3] Zhou C S and Chen T L 1997 *Phys. Lett. A* **225** 60
[4] Colli E, Piassi V S M, Tufaile A and Sartorelli J C 2004 *Phys. Rev. E* **70** 066215
[5] Hassell M 1975 *J. Anim. Ecol.* **44** 283
[6] Andrecut M and Kauffman S A 2007 *Phys. Lett. A* **367** 281
[7] Ge H X 2011 *Chin. Phys. B* **20** 090502
[8] Yuen C H and Wong K W 2012 *Chin. Phys. B* **21** 010502
[9] Zhusubaliyev Z T and Mosekilde E 2003 *Bifurcations and Chaos in Piecewise-Smooth Dynamical Systems* (Singapore: World Scientific)
[10] Bao B C, Kang Z S, Xu J P and Hu W 2009 *Acta Phys. Sin.* **58** 1420 (in Chinese)
[11] Wiggins S 2003 *Introduction to Applied Nonlinear Dynamical Systems and Chaos* (New York: Springer)
[12] Guckenheimer J and Holmes P 2002 *Nonlinear Oscillations, Dynamical Systems, and Bifurcations of Vector Fields* (New York: Springer)
[13] Li X F, Chu Y D and Zhang H 2012 *Chin. Phys. B* **21** 030203
[14] Schuster H G and Just W 2005 *Deterministic Chaos, an Introduction* (Weinheim: WILEY-VCH)